

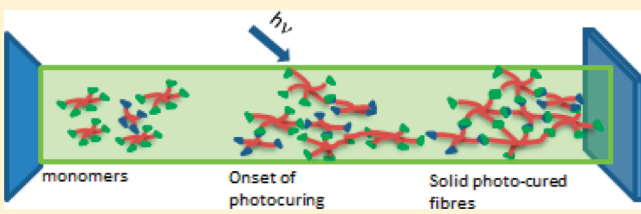
Thiol–Ene Chemistry: A Greener Approach to Making Chemically and Thermally Stable Fibers

Kadhiravan Shanmuganathan,[†] Robert K. Sankhagowit,[†] Prashanth Iyer,[†] and Christopher J. Ellison^{*,†,‡}

[†]Department of Chemical Engineering and [‡]Texas Materials Institute, University of Texas Austin, 1 University Station C0400, Austin, Texas 78712, United States

 Supporting Information

ABSTRACT: Fibers of micrometer and submicrometer diameters have been of significant interest in recent years owing to their advanced applications in diverse fields such as optoelectronics, regenerative medicine, piezoelectrics, ceramic materials, etc. There are a number of processes to make thin fibers including electrospinning, melt blowing, and recently developed Forcespinning. However, use of solvents or heat to lower viscosity for processing is common to all existing polymer fiber manufacturing methods, and a greener approach to making fibers remains a challenge. Interestingly, nature has engineered spiders and silkworms with a benign way of making mechanically strong and tough fibers through an intricate self-assembly of protein constituents during the fiber formation process. Comprehending the biosynthetic process and precisely replicating it has been a challenging task. However, we find that extruding small functional segments into solid fibrillar structures, through mediation of chemical interactions between the subunits, is a design approach that can be broadly adapted from nature to realize a greener fiber manufacturing process. Using the robust chemistry of thiol–ene photopolymerization, we demonstrate here that a photocurable mixture of a multifunctional acrylate, a tetrafunctional thiol, and a photoinitiator can be processed into continuous fibers by *in situ* photopolymerization during electrospinning under ambient conditions. The fibers are mechanically robust and have excellent chemical and thermal stability. While electrospinning has been used to demonstrate this concept, the chemistry could be broadly adapted into other fiber manufacturing methods to produce fibers without using solvents or heat.



KEYWORDS: green chemistry, thiol–ene, fibers, electrospinning, photopolymerization, silk

INTRODUCTION

Significant advancements in fiber production techniques have facilitated new applications for fibrous materials in diverse fields such as optoelectronics,¹ regenerative medicine,² piezoelectrics,³ ceramic materials,⁴ etc. Electrospinning,⁵ melt blowing,⁶ and Forcespinning⁷ are currently popular for their capabilities to yield thin fibers ranging from several tens of nanometers to many micrometers with relatively straightforward tunability. Electrospinning requires application of a strong electric field (10–20 kV) to a polymer–solvent solution, to draw a filament extruded from an orifice. At a critical voltage the electrostatic repulsive forces in the solution overcome surface tension forces and a jet of polymer solution is driven toward a grounded collector. Rapid evaporation of solvent into the surrounding environment leaves behind solid polymer fibers on the collector.^{5,8} Although the technique is very versatile which has resulted in extensive use in research, it is used sparsely in industrial production. Regardless, electrospinning usually employs large quantities of volatile solvent (i.e., 80–95 wt %) and presents challenges such as solvent recycling/recovery, toxicity of solvents, and a low mass throughput due to solvent evaporation.⁹ Alternatively, polymer melts have been used in place of solutions.¹⁰ However, the melt electrospinning process is constrained by high viscosities and low conductivities of polymer melts and the need for a high temperature environment.

Alternatives to electrospinning include melt blowing, where molten polymer is extruded through a nozzle and stretched into continuous filaments with jets of hot air to yield very thin fibers, often exceeding 1–2 μm diameter. Significant thermal energy is needed both for melting the polymer and sustaining the continuous hot air jet that attenuates the molten fiber. Very recently a new technique called either Forcespinning⁷ or rotary jet spinning¹¹ has been developed which uses centrifugal force to stretch fibers by spinning a polymer solution or melt through a rotating nozzle. This process can have a much higher fiber production rate relative to electrospinning. In the three synthetic fiber manufacturing processes discussed so far, large quantities of solvent or thermal energy input are required for lowering viscosity to enable processing of polymers into fine fibers.

Conversely, spiders and silkworms have developed benign ways of making silk fibers with high strength and toughness.¹² Significant advancements have been made in shedding light on silk formation processes.^{13,14} Obtaining a complete and fundamental understanding of this biosynthetic process, or engineering synthetic silk fibers with equivalent mechanical properties, is an open challenge in the field.¹² A recent study¹⁵ has found that

Received: May 27, 2011

Revised: September 26, 2011

Published: October 12, 2011

spiders achieve fiber formation by rapid triggering of multivalent ionic bonds at the terminal end of proteins in a very location specific manner (i.e., only inside the spinning duct, not in the spinning gland which serves as the protein reservoir) leading to strong association of the protein ends. Viewed broadly, nature's approach of chemically linking small functional units into long chain molecules and solid fibrillar structures while simultaneously extruding the fibers is fundamentally different from current synthetic fiber manufacturing methods, where extrusion of preformed long chain polymers is facilitated with organic solvent or heat. Drawing inspiration from nature's approach, extruding small reactive subunits and polymerizing them en route to fiber formation could be a way to make fibers without solvents or heat. Identifying a suitable chemistry where chemical interactions between small reactive molecules can be rapidly triggered during typical synthetic fiber extrusion speeds ($>1\text{ m/s}$), which is orders of magnitude faster than rates at which spiders spin silk ($1\text{--}10\text{ cm/s}$),¹⁶ is a challenge. However, we determined that thiol–ene chemistry, triggered by exposure to light, can achieve this requirement due to its extremely fast kinetics under ambient conditions (i.e., air and room temperature environment). While there have been a few previous attempts of photocuring electrospun fibers, preformed fibers have been postcured¹⁷ or the processing step itself required solvents to dissolve the photocurable polymer.¹⁸ In another example, Kim et al. partially converted volatile monomers to oligomers by application of heat prior to spinning fibers with *in situ* photopolymerization.¹⁹

Thiol–ene photopolymerizations typically follow a step-growth radical polymerization mechanism involving a multi-functional *thiol* and a wide variety of *enes*.²⁰ The photoinitiator, activated by light, abstracts a hydrogen atom from a *thiol* forming a thiyl radical. The thiyl radical then propagates by attacking the alkene group. This is followed by chain transfer of the carbon-centered radical to another *thiol* functional group, forming a thioether linkage and regeneration of a thiyl radical. The successive propagation/chain transfer mechanism forms the basis for an ideal step growth polymerization under some circumstances. Termination occurs by the coupling of any two radical species.²¹ However in cases where the *ene* monomer readily homopolymerizes (e.g., acrylates, methacrylates, or vinyl benzenes) there is a competition between step growth and chain growth polymerizations.²⁰ In such cases, vinyl groups will be consumed by both homopolymerization and propagation/chain transfer with thiols, and using a 1:1 stoichiometric mixture of *thiol* to *ene* results in less conversion of *thiol* compared to *ene*. To achieve roughly equivalent conversion of functional groups, the stoichiometry should be appropriately adjusted (further explanation can be found in the Results and Discussion section).

The many advantages associated with thiol–ene photopolymerizations such as fast polymerization rates in air, low shrinkage at high conversion, network homogeneity, and versatility in *ene* selection,²⁰ has extended the use of thiol–ene chemistry into a broad range of applications including nanoimprinting,²² dental restorative materials,²³ extracellular matrix mimics,²⁴ hydrogels for protein delivery,²⁵ and gas transport membranes.²⁶ Thiol–ene photopolymerizations have a distinct advantage over traditional acrylic photopolymerizations in that they are not significantly inhibited by oxygen and are generally polymerizable without additional photoinitiator molecules.²⁷ However, adding a photoinitiator can greatly enhance the rate of polymerization. We demonstrate here for the first time that precursors with reactive *thiol* and *ene* functional groups could be *in situ* photopolymerized

during the electrospinning process to produce fibers, without the use of heat, solvents, or other volatile components.

EXPERIMENTAL SECTION

Materials. Pentaerythritol tetrakis (3-mercaptopropionate) (PETT) (boiling point: $519.9\text{ }^{\circ}\text{C}$ at 760 mmHg) was purchased from Sigma Aldrich. Dipentaerythritol pentaacrylate (DPPA) (boiling point: $619.6\text{ }^{\circ}\text{C}$ at 760 mmHg) was kindly donated by Sartomer USA. Irgacure 2100 was provided by BASF, Switzerland. All chemicals were used as received.

Electrospinning Apparatus. The electrospinning apparatus (Figure 1) consists of a high voltage DC supply (Gamma High Voltage Research ES40P, Florida), a syringe pump (Chemex Fusion 200), and a grounded copper plate as a collector. The area from the needle tip to the collector was encased in a Plexiglas box capable of blocking ultraviolet radiation from reaching the operator. Light for photocuring was provided by a Scopelite 200 (Optical Building Blocks), which has a metal halide lamp with spectral output ranging between $350\text{--}700\text{ nm}$. The light guide was fitted with a collimating lens to provide a more focused beam for photocuring the fibers.

Electrospinning. For electrospinning, PETT and DPPA were mixed together in ratios of 1:3.4, 1:4.4, or 1:5.6 along with 6 wt % (on total weight of *thiol* and acrylate) of Irgacure 2100 (photoinitiator) in a vibratory mixer (Thermolyne 37600) for about 5 min. The solution was prepared in an environment that minimized UV light and was then loaded into a syringe that was masked from room light and fitted with a blunt needle (0.8 mm inner diameter). Positive charge was applied to the needle, and the other end was grounded to a copper plate target. The solution was fed at 10 mL/h , and once a drop was observed at the needle tip, a 18 kV potential was applied that stretched the drop into an elongated filament jet which moved toward the grounded collector placed 14 cm from the needle tip. The light was positioned at a distance of about 3 in. from the collector and at an angle such that it illuminated both the jet near the collector and the collector. Intensity of the light at 3 in. distance was measured with a radiometer and found to be $\sim 200\text{ mW/cm}^2$.

Fourier Transform Infrared Spectroscopy (FTIR). The curing kinetics of the thiol–ene mixtures were determined using a Nicolet Magna-IR 550 FTIR spectrometer with a KBr beam splitter and DTGS KBr detector. Real time scans were conducted in transmission mode at the rate of approximately 5 spectra/second, averaging 2 scans/spectrum. A drop of the photocurable mixture consisting of measured amounts of *thiol*, acrylate, and photoinitiator was placed on a NaCl crystal and spread into a thin film $20\text{--}30\text{ }\mu\text{m}$ thick using a glass slide. The thickness of the film was targeted specifically to closely match the diameter of an average fiber made in this study. Sample preparations were performed in a room with no stray UV light and then loaded into the FTIR chamber which was continuously purged with zero grade air. The scans were conducted isothermally at $25\text{ }^{\circ}\text{C}$. To ensure that the photocuring conditions in the FTIR experiment were nearly identical to those in the fiber spinning process, the same light source (Optical Building Blocks Scopelite 200), positioning distance (3 in.), and collimating lens were used. Samples were irradiated until the reaction was complete, i.e. until the double bond (1630 cm^{-1}) and thiol absorption (2570 cm^{-1}) peaks reached a constant height. Double bond conversion at a given time was determined from the peak areas (normalized to another peak area that is unaffected by photopolymerization) before and during polymerization as follows

$$\text{degree of conversion} = (A_0 - A_t)/A_0 \quad (1)$$

where A_0 and A_t refer respectively to the normalized carbon double bond peak area before polymerization and the normalized carbon double bond peak area at any given time t .

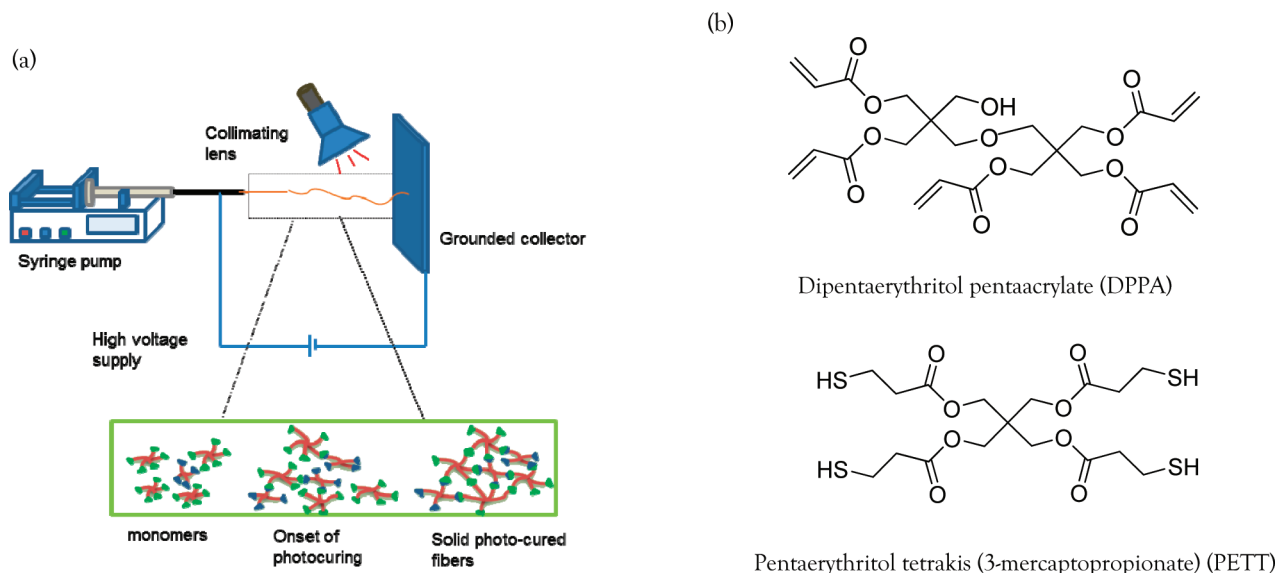


Figure 1. (a) Schematic of the electrospinning set up with UV light source for *in situ* photopolymerization of thiol–ene compounds during fiber spinning. (b) Chemical structures of dipentaerythritol pentaacrylate (DPPA) and pentaerythritol tetrakis(3-mercaptopropionate) (PETT) used to demonstrate this thiol–ene based solventless fiber spinning process.

Scanning Electron Microscopy (SEM). Fiber morphology and diameter distribution was determined by SEM analysis. Fibers were affixed to the SEM sample holder with carbon tape and sputter coated with Au–Pd target. Samples were scanned at an accelerating voltage of 15 KV, and the images were analyzed by ImageJ software. Fiber diameter distribution was obtained by measuring diameters of 110 fibers from 7 different images.

Dynamic Mechanical Analysis (DMA). The thermomechanical and stress–strain behavior of the fibers was determined using a DMA (TA Instruments Q800). Single fibers were tested in dynamic tensile mode using a temperature sweep method at a fixed frequency of 1 Hz. Temperature was ramped from 25 to 200 °C @ 3 °C/min with a sample preload force of 0.01 N and an amplitude of 15 μ m. Stress–strain tests were also conducted on single fibers in DMA strain rate mode. Samples were tested isothermally at 25 °C using a preload force of 0.01 N and a strain rate of 500 μ m/min, which was roughly 5% of the gauge length of fibers. The fiber diameter and quality of the test specimens were evaluated by optical microscopy before mechanical tests.

Chemical and Thermal Stability of Fibers. Chemical resistance of fibers was evaluated by immersing the fibers in toluene or tetrahydrofuran for 4 h at 50 °C. Thermogravimetric analysis was also carried out on the fibers in nitrogen atmosphere. Fiber samples were heated up to 1000 at 20 °C/min to characterize thermal stability.

RESULTS AND DISCUSSION

Figure 1a shows an apparatus schematic for photopolymerizing thiol–ene groups during the electrospinning process. Integrating thiol–ene photopolymerization and electrospinning into a simultaneous process presents several operational challenges. The curing kinetics must be matched to the speed of the high velocity fluid jet moving toward the collector. Reneker et al.⁵ reported the jet velocity to be \sim 0.5 m/s. We have estimated our average jet velocity at the collector as \sim 1 m/s, based on known feed rates and typical starting and final fiber diameters. Considering this speed and the distance between the needle tip and collector, the available time for photopolymerizing the thiol–ene fluid jet *in situ* is \sim 0.1 s. Hence, a very high speed curing system is necessary, which is an important advantage of thiol–ene over

other chemistries. In order to ensure sufficient *in situ* photopolymerization of *thiol* and *enes* within 0.1 s, we chose to use multifunctional components including a pentafunctional acrylate (dipentaerythritol pentaacrylate; DPPA) and a tetrafunctional thiol (3-mercaptopropionate; PETT) shown in Figure 1b. Irgacure 2100, a phosphine oxide photoinitiator, was used to facilitate high speed photopolymerization and was miscible with all mixtures used in this study.

Producing defect free fine fibers in electrospinning requires careful consideration of both the surface tension and viscoelasticity of the spinning fluid.²⁸ While low viscosities aid rapid attenuation of the fiber they can promote droplet formation due to surface tension driven breakup of the fluid jet (electrospraying). On the other hand, high viscosity fluids resist the attenuation process resulting in thicker fibers. For reference, the viscosity range of polymer melts used in electrospinning and melt blowing are typically between 1 and 100 Pa·s.²⁹ The viscosity of the spinning mixture here depends on the viscosity of the *thiol* and *ene* components and their ratio in the mixture. Since the *thiol* to *ene* group ratio in the mixture also has a significant effect on curing kinetics and physical properties, the composition must be carefully chosen to optimize both curing speed and viscosity. In a thiol–acrylate system, acrylates tend to homopolymerize faster than reacting with *thiol* groups. As a result, a 1:1 molar ratio of *thiol*:*ene* groups often results in incomplete conversion of *thiol* functional groups. Previous studies in thiol–acrylate systems have shown that a 1:4 ratio of *thiol* to *ene* groups can lead to roughly equivalent conversion of both functional groups.²⁷ We investigated a set of mixtures close to this ratio, to find a composition with suitable viscosity and curing speed. Continuous and nonporous fibers (Figure 2) were achieved reproducibly by electrospinning a mixture of DPPA and PETT with a 1:4.4 ratio of *thiol* to *ene* groups. These fibers were obtained by simply mixing DPPA and PETT in the previously mentioned ratio, along with 6 wt % Irgacure 2100 as photoinitiator, for 5 min and electrospinning them through a syringe needle (0.8 mm inner diameter). Fibers free of bead defects were obtained at the

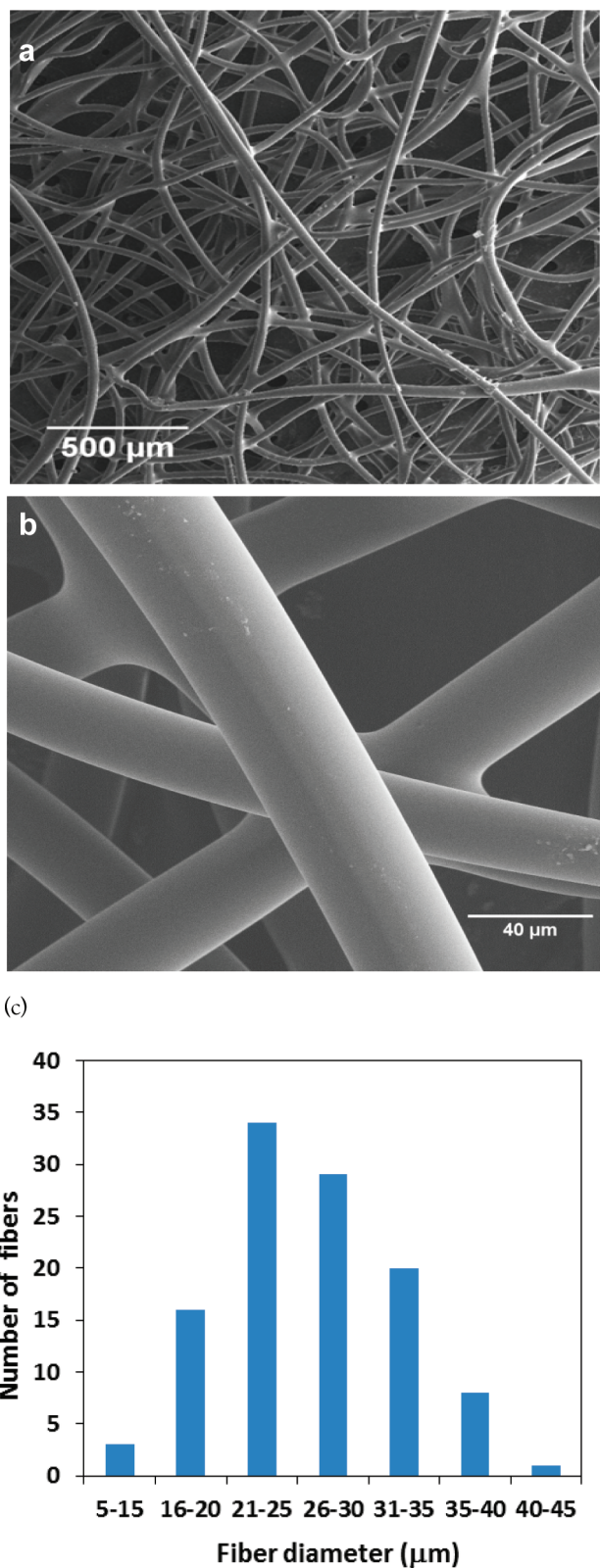


Figure 2. (a) Low and (b) high magnification SEM images of thiol–ene fibers made by photopolymerization of PETT and DPPA in a 1:4.4 *thiol* to *ene* ratio along with 6 wt % Irgacure 2100 as photoinitiator. (c) Diameter distribution of fibers.

grounded collector (positioned 14 cm from needle tip) by electrospinning at a potential of 18 kV and a feed rate of

10 mL/h. As the thiol–ene mixture emerging from the needle approached the grounded collector, it was photopolymerized with a UV light source (Optical Building Blocks Scopelite 200, 350–700 nm, at an intensity of 200 mW/cm² at the fiber location) with the collimator positioned about 3 in. from the collector at an angle such that the light illuminated both the jet near the collector and the fiber collection point itself. This positioning is important to yield solid well-cured fibers through efficient and timely curing of thiol–ene functionalities. Curing the fluid filament closer to the needle tip can limit stretching of the polymer resulting in thicker fibers, while curing closer to the collector could result in significant bead formation from surface tension driven fiber breakup or flow of fibers depositing on the collector. The 1:4.4 DPPA:PETT mixture was viscous enough to produce a continuous fluid jet which had a sufficiently high curing speed to yield solid fibers on the collector that were nearly free of defects. Figure 2c shows fiber diameters of 8–45 μm with an average diameter of about 25 μm .

When the stoichiometry of *thiol* to *ene* is slightly altered, we observed quite significant changes in fiber morphology, such as partially cured discontinuous strands and other defects [Supporting Information Figure 1]. In order to accomplish *in situ* photopolymerization of thiol–ene units within the very short flight time (<0.5 s) of the jet before it hits the collector, the curing kinetics of thiol–ene units must be equally as fast. The entire fiber formation and solidification process herein is most appropriately viewed as a simultaneous interplay of several physical and chemical factors including fluid viscoelasticity, surface tension, electrostatic forces, and curing kinetics. For example, electrostatic repulsive forces tend to increase the surface area of the electrified jet originating from the needle tip, while surface tension can induce the elongated jet to break into spheres to minimize surface area; high viscosities can limit rapid diameter reduction, while low viscosities facilitate it.

To investigate the effect of *thiol* to *ene* ratio on curing kinetics, real time infrared spectroscopy experiments were performed in ambient air (see the Experimental Section). Figure 3 shows the photocuring kinetics of the different mixtures of thiol–ene described above. It is important to note that approximately 40–50% double bond conversion is achieved in less than a second (Figure 3b) which is a crucial aspect for the fiber spinning process and consistent with typical conversions of 55–60% observed in the final collected fibers as determined by IR. Though the final conversion of *ene* groups and the complete kinetics are roughly similar at first glance (Figure 3a), there is a significant difference at very short curing times, i.e., less than 2 s (Figure 3b). In this time scale, it is clear that increasing *thiol* content leads to faster cure. Since the time available for curing the thiol–ene filament en route to the collector is fractions of a second, slight kinetic differences in this regime likely have significant impact on fiber quality. In addition, the PETT *thiol* used here is less viscous than the DPPA *ene*. The viscosity of the thiol–ene mixture with a 1:4.4 ratio of *thiol* to *ene* groups that yielded high quality fibers is about 1.7 Pa·s. A lesser *thiol* content of 1:5.6 increases the viscosity to 2.1 Pa·s, while increasing the *thiol* content to 1:3.4 decreases the viscosity to 1.3 Pa·s [Supporting Information Figure 2]. Supporting Information Figure 1 shows SEM images of fibers produced with thiol–ene ratios of 1:3.4 and 1:5.6. The observed fiber morphology is consistent with dominant surface tension forces and relatively low viscosity and curing speed. When the *thiol* content is less (1:5.6 *thiol*:*ene*), the viscosity is sufficient to resist deformation

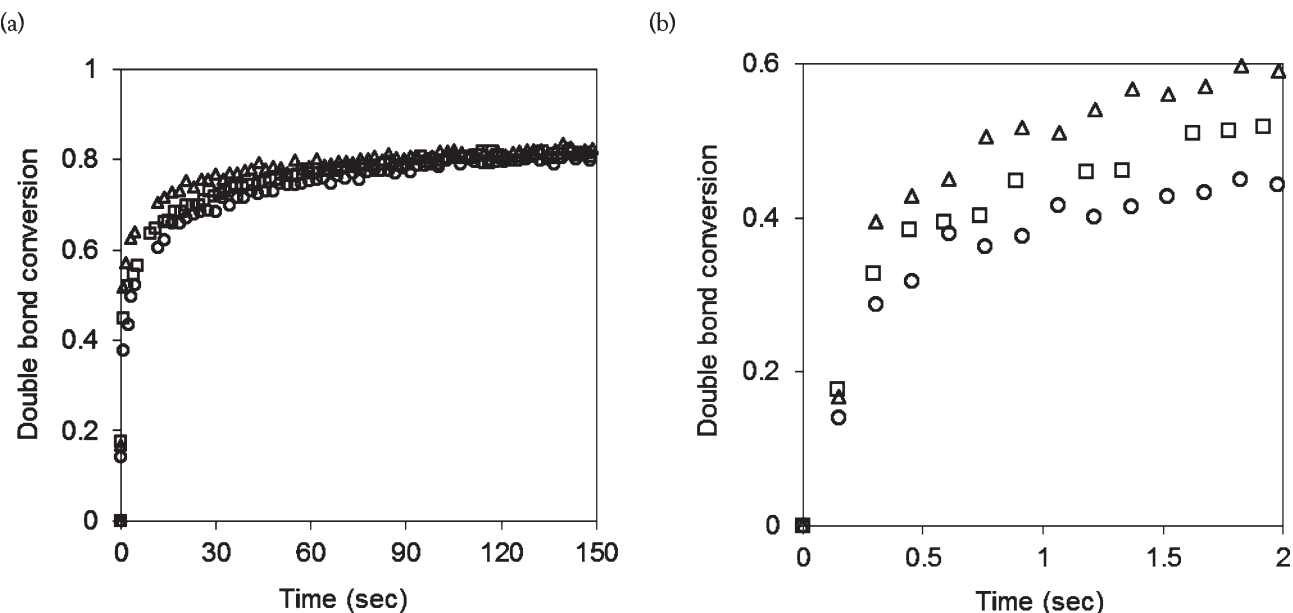


Figure 3. (a) Double bond conversion by real time FTIR spectroscopy measurements taken in air for the photopolymerization of PETT and DPPA of different thiol:ene ratios based on: thiol:ene = 1:5.6 (open circles), thiol:ene = 1:4.4 (open squares), thiol:ene = 1:3.4 (open triangles). (b) Data in part (a) replotted to show the kinetics of curing in the first few seconds of light exposure. Curing speed increases with increase in thiol content to 40–50% double bond conversion in less than a second. Samples irradiated at $\sim 200 \text{ mW/cm}^2$ using 6 wt % Irgacure 2100 as photoinitiator. (Data collected approximately every 0.15 s. For clarity every 10th data point has been plotted in part (a)).

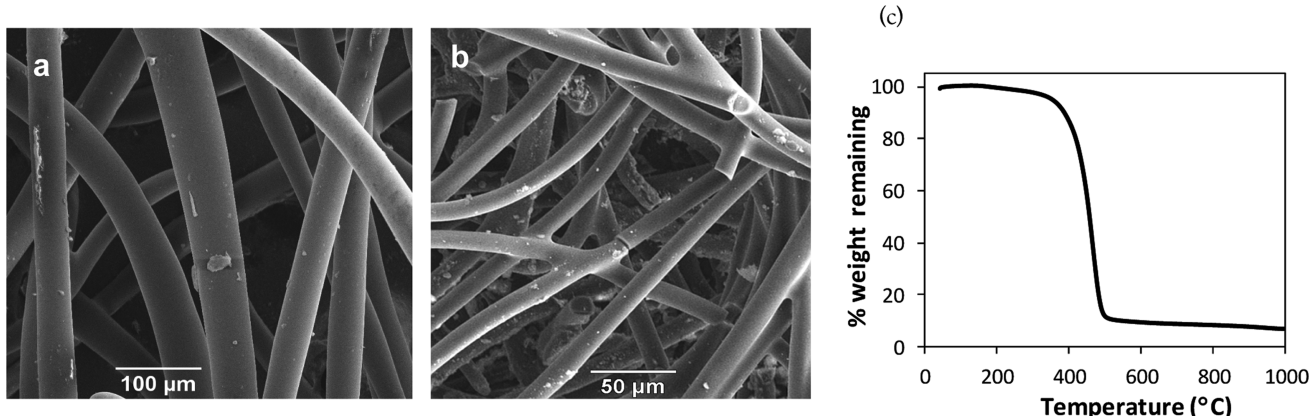


Figure 4. (a) SEM images of thiol–ene fibers that were exposed to toluene at 50 °C for 4 h. The fibers remained intact and largely unaffected demonstrating the excellent chemical stability. (b) SEM images of residual thiol–ene fibers after heating in nitrogen in the TGA to 1000 °C. These fibers were made by photopolymerization of PETT and DPPA in a 1:4.4 thiol to ene ratio along with 6 wt % Irgacure 2100 as photoinitiator. (c) Thermogravimetric analysis of the thiol–ene fibers in nitrogen showing no significant weight loss up to 400 °C.

by surface tension forces but the photocuring kinetics are slower leading to partially cured material hitting the collector and causing defects in the fibers.

When the thiol content is increased (1:3.4), photocuring kinetics are fast enough, but the lower viscosity leads to defects in fibers. Such defects were not observed with a 1:4.4 ratio of thiol to ene, which had the right balance of viscosity and curing kinetics to yield well-cured solid fibers as shown in Figure 2.

Reduction in the thiol content below a certain level also reduces photocuring rates in air and ultimately adversely affects final fiber quality. In traditional acrylate photopolymerizations, oxygen reacts with carbon radicals to form peroxy radicals. Peroxy radicals are less reactive than carbon radicals, and therefore oxygen quenches the

reaction. In a thiol–ene photopolymerization, the peroxy radical abstracts hydrogen from a thiol unit regenerating thiyl radicals making thiol–ene polymerizations less sensitive to oxygen.²⁷ This feature is instrumental in performing this fiber forming process in ambient conditions, and it could be an important controlling factor in fiber quality in some circumstances.

Our laboratory is currently building upon this research to generate submicrometer-diameter fibers. To the best of our knowledge, this is the first report of using the chemistry of thiol–ene photopolymerization to enable more environmentally friendly fiber spinning processes. Given that the science of both electrospinning and thiol–ene chemistry is very versatile and tunable, a more detailed and systematic investigation into factors

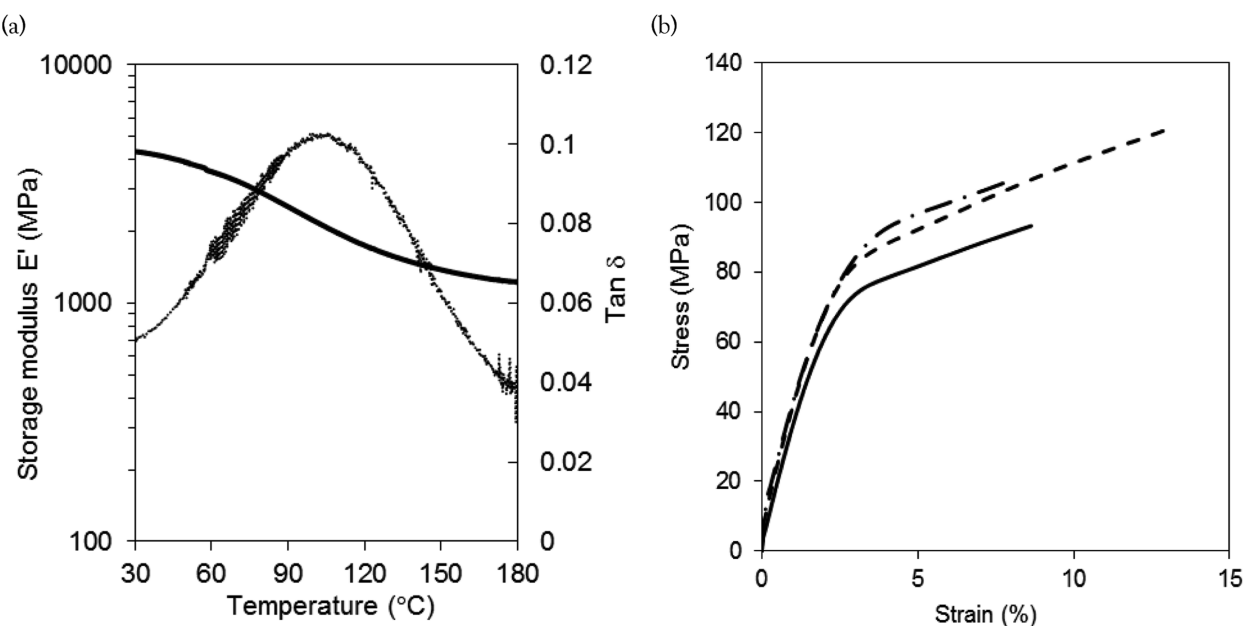


Figure 5. (a) DMA of thiol–ene fibers showing the storage modulus (E') (solid line) and $\tan \delta$ (dotted line) as a function of temperature. The fibers have a storage modulus more than 1000 MPa even above the glass transition temperature (~ 100 $^{\circ}\text{C}$) owing to the presence of covalent cross-links. All 3 samples that were tested exhibited identical behavior and a representative trace is shown above. (b) Stress–strain behavior of 3 thiol–ene fibers tested in tensile mode. In spite of chemical cross-linking, the fibers have an elongation at break of 8–12%. These fibers were made by photopolymerization of PETT and DPPA in a 1:4.4 *thiol* to *ene* ratio along with 6 wt % Irgacure 2100 as photoinitiator.

Table 1. Chart Comparing the Characteristics of This Thiol–Ene Fiber Spinning Route with Electrospinning (Solution or Melt)

features	fiber spinning by thiol–ene photopolymerization	solution electrospinning	melt electrospinning
productivity	~ 10 g/h	~ 0.5 – 2.0 g/h ^a	~ 10 g/h
solvent requirement	none	for every 100 g of fibers 0.4 to 1.9 L solvent required	none
potential for residual solvents in the end product	none	yes	none
heat input	none	sometimes necessary to dissolve polymer	requires significant thermal energy

^a Assuming a 10 mL/h feed rate, single nozzle, and 5–20 wt % polymer solution for solution electrospinning.

affecting the fiber formation process will be critical to identify conditions that produce thinner fibers such as nanofibers.

It is important to note that the chemistry and method used to make fibers in this work are quite different from the biosynthetic process in spiders and silk worms. However, the objective was not to replicate spider silk fibers but to create a greener fiber spinning route through simultaneous polymerization and extrusion, a process analogous to that of spiders and silk worms. While the biosynthetic process involves self-assembly through secondary interactions, the fiber formation reported here relies on externally triggering covalent interactions between functional segments. This has several significant advantages. The fibers have very good chemical stability because of the cross-linked molecular architecture formed during curing. For example, thiol–ene fibers were not soluble or fractured by swelling in THF or toluene, which are good solvents for the *ene* and *thiol* precursors. Further, the morphology of the fibers was unaffected even after immersing the fibers in toluene at 50 $^{\circ}\text{C}$ for 4 h. (Figure 4a), indicating that the fibers were well-cured with a cross-linked

structure. Additionally, the fibers demonstrated negligible weight loss when heated up to 400 $^{\circ}\text{C}$ in nitrogen (Figure 4c). Upon heating to 1000 $^{\circ}\text{C}$ in nitrogen, the fibers were converted to carbonaceous material but still retained their cylindrical geometry (Figure 4b).

Another impressive aspect of these fibers is their thermomechanical properties. Figure 5a shows the storage modulus (E') of these fibers as a function of temperature. The fibers exhibited a room temperature modulus of about 4–5 GPa and a glass transition temperature of about 100 $^{\circ}\text{C}$ ($\tan \delta$ peak temperature). Differential Scanning Calorimetry also shows a glass transition around 90 $^{\circ}\text{C}$. As would be expected for a cross-linked network, the modulus did not drop drastically at the glass transition and was more than 1000 MPa even at temperatures close to 200 $^{\circ}\text{C}$. Apart from superior thermomechanical stability, the fibers also had good ultimate tensile properties. Single fiber tensile tests in Figure 5b showed that the fibers have a reasonably good elongation at break (8–12%) and ultimate tensile strength around 80–120 MPa. Unlike the dynamic elastic modulus, ultimate tensile properties are more sensitive to

microscopic sample defects which can affect consistency of results across different batches of fibers in ways that more traditional tensile bars are less susceptible to. Nonetheless, these results are consistent with or slightly better than those reported for other thiol–acrylate films³⁰ and show that the fibers have a reasonably good stretchability, which is also confirmed qualitatively while handling them.

The productivity and environmentally friendly aspects of the process relative to solution or melt electrospinning are compared in Table 1. Apart from being a solventless, energy efficient process, the use of thiol–ene chemistry presents many advantages.

In conclusion, the rapid thiol–ene photopolymerization process outlined in this research can be used to produce fibers easily in ambient conditions without application of any solvent or heat. Thiol–ene chemistry provides wide latitude in the choice of compatible functionalities for a wide-range of applications. Though we have used electrospinning in this demonstration, this chemical approach to fiber manufacturing should be broadly applicable in other batch or continuous fiber producing methods to create fibers with superior thermal and chemical stability and robust mechanical properties.

■ ASSOCIATED CONTENT

Supporting Information. SEM images and rheology of thiol–ene mixtures. This material is available free of charge via the Internet at <http://pubs.acs.org>.

■ AUTHOR INFORMATION

Corresponding Author

*Phone: 512-471-6300. E-mail: ellison@che.utexas.edu.

■ ACKNOWLEDGMENT

The authors wish to acknowledge Dr. Benny Freeman for allowing use of his DMA, Brandon Rawlings for help with FTIR studies, and Dr. Dustin Janes for reading the manuscript and giving valuable suggestions. C.J.E. gratefully acknowledges partial funding for the research from the Welch Foundation (grant #F-1709).

■ REFERENCES

- (1) Kumar, A.; Jose, R.; Fujihara, K.; Wang, J.; Ramakrishna, S. *Chem. Mater.* **2007**, *19*, 6536.
- (2) Beachley, V.; Wen, X. J. *Prog. Polym. Sci.* **2010**, *35*, 868.
- (3) Egusa, S.; Wang, Z.; Chocat, N.; Ruff, Z. M.; Stolyarov, A. M.; Shemuly, D.; Sorin, F.; Rakich, P. T.; Joannopoulos, J. D.; Fink, Y. *Nat. Mater.* **2010**, *9*, 643.
- (4) Wideman, T.; Sneddon, G. L. *Chem. Mater.* **1996**, *8*, 3.
- (5) Reneker, D. H.; Yarin, A. L.; Fong, H.; Koombhongse, S. *J. Appl. Phys.* **2000**, *87*, 4531.
- (6) Ellison, C. J.; Phatak, A.; Giles, D. W.; Macosko, C. W.; Bates, F. S. *Polymer* **2007**, *48*, 3306.
- (7) Sarkar, K.; Gomez, C.; Zambrano, S.; Ramirez, M.; de Hoyos, E.; Vasquez, H.; Lozano, K. *Mater. Today* **2010**, *13*, 12.
- (8) Shin, Y. M.; Hohman, M. M.; Brenner, M. P.; Rutledge, G. C. *Appl. Phys. Lett.* **2001**, *78*, 1149.
- (9) Zhou, H. J.; Green, T. B.; Joo, Y. L. *Polymer* **2006**, *47*, 7497.
- (10) Lyons, J.; Li, C.; Ko, F. *Polymer* **2004**, *45*, 7597.
- (11) Badrossamay, M. R.; McIlwee, H. A.; Goss, J. A.; Parker, K. K. *Nano Lett.* **2010**, *10*, 2257.
- (12) Omenetto, F. G.; Kaplan, D. L. *Science* **2010**, *329*, 528.
- (13) Jin, H. J.; Kaplan, D. L. *Nature* **2003**, *424*, 1057.
- (14) Silvers, R.; Buhr, F.; Schwalbe, H. *Angew. Chem., Int. Ed.* **2010**, *49*, 5410.
- (15) Hagn, F.; Thamm, C.; Scheibel, T.; Kessler, H. *Angew. Chem., Int. Ed.* **2011**, *50*, 310.
- (16) Guess, K. B.; Viney, C. *Thermochim. Acta* **1998**, *315*, 61.
- (17) Tan, A. R.; Iakovits, J. L.; Baker, B. M.; Brey, D. M.; Mauck, R. L.; Burdick, J. A. *J. Biomed. Mater. Res. Part A* **2008**, *87A*, 1034.
- (18) Gupta, P.; Trenor, S. R.; Long, T. E.; Wilkes, G. L. *Macromolecules* **2004**, *37*, 9211.
- (19) Kim, S. H.; Nair, S.; Moore, E. *Macromolecules* **2005**, *38*, 3719.
- (20) Hoyle, C. E.; Lee, T. Y.; Roper, T. J. *J. Polym. Sci., Polym. Chem.* **2004**, *42*, 5301.
- (21) Morgan, C. R.; Magnotta, F.; Ketley, A. D. *J. Polym. Sci., Polym. Chem.* **1977**, *15*, 627.
- (22) Hagberg, E. C.; Malkoch, M.; Ling, Y. B.; Hawker, C. J.; Carter, K. R. *Nano Lett.* **2007**, *7*, 233.
- (23) Lu, H.; Carioscia, J. A.; Stansbury, J. W.; Bowman, C. N. *Dent. Mater.* **2005**, *21*, 1129.
- (24) Fairbanks, B. D.; Schwartz, M. P.; Halevi, A. E.; Nuttelman, C. R.; Bowman, C. N.; Anseth, K. S. *Adv. Mater.* **2009**, *21*, S005.
- (25) Aimetti, A. A.; Machen, A. J.; Anseth, K. S. *Biomaterials* **2009**, *30*, 6048.
- (26) Kwisnek, L.; Nazarenko, S.; Hoyle, C. E. *Macromolecules* **2009**, *42*, 7031.
- (27) Cramer, N. B.; Scott, J. P.; Bowman, C. N. *Macromolecules* **2002**, *35*, 5361.
- (28) Fong, H.; Chun, I.; Reneker, D. H. *Polymer* **1999**, *40*, 4585.
- (29) (a) Dalton, P. D.; Grafahrend, D.; Klinkhammer, K.; Klee, D.; Moller, M. *Polymer* **2007**, *48*, 6823. (b) Tan, D. H.; Zhou, C. F.; Ellison, C. J.; Kumar, S.; Macosko, C. W.; Bates, F. S. *J. Non-Newton. Fluid Mech.* **2010**, *165*, 892.
- (30) Senyurt, A. F.; Wei, H.; Hoyle, C. E.; Piland, S. G.; Gould, T. E. *Macromolecules* **2007**, *40* (14), 4901–4909.